JOURNAL OF AGRICULTURAL AND FOOD CHEMISTRY

Studies on Water Transport through the Sweet Cherry Fruit Surface. 10. Evidence for Polar Pathways across the Exocarp

HOLGER WEICHERT AND MORITZ KNOCHE*

Institut für Acker- und Pflanzenbau, Martin-Luther-Universität Halle-Wittenberg, 06099 Halle (Saale), Germany

Water uptake through the fruit surface is considered as an important factor in cracking of sweet cherry (*Prunus avium* L.) fruit. Uptake may occur by diffusion and/or viscous flow along a polar pathway. To establish the mechanism of water uptake, the effects of viscosity and molecular weight of selected osmotica on water uptake into detached sweet cherry fruit were investigated. In addition we investigated the effect of temperature on penetration of 2-(1-naphthyl)[1-^{14}C]acetic acid ([^{14}C]NAA; pK_a = 4.2) as a molecular probe in the nondissociated (pH 2.2) and dissociated (pH 6.2) forms. Rates of water uptake were linearly related to the inverse viscosity of gum arabic solutions (range of concentrations and dynamic viscosities 10−300 g L^{-1} and 1.3 × 10^{-3} to 115.9 × 10^{-3} Pa s, respectively). When fruit was incubated in solutions of osmotica of differing molecular weight that were isotonic to the fruit's water potential, water uptake depended on the molecular weight of the osmoticum [range 58−6000 for NaCl to poly(ethylene glycol) 6000 (PEG 6000)]. There was no uptake from PEG 6000 solutions, but rates of water uptake increased as the molecular weight of the osmotica decreased. Apparent water potentials of sweet cherry fruit, determined by incubating fruit in concentration series of selected osmotica, increased as the molecular weight of the osmotica increased up to 1500 and remained constant between 1500 and 6000. Reflection coefficients (σ) estimated from this relationship were closely related to hydrodynamic radii (r) of the osmotica [$\sigma = 1.0(\pm 0.0) - [10.9(\pm 0.9) \times 10^{-11}][r^{-1}\ (m^{-1})]$, $R^2 = 0.97$, $P < 0.0001$]. The permeability of the sweet cherry fruit exocarp to NAA (pK_a = 4.2) and temperature dependence of NAA permeability (P_d) as indexed by the energy of activation (E_a, temperature range 5−35 °C) were significantly higher for the nondissociated NAA (pH 2.2, $P_d = 10.2(\pm 0.8) \times 10^{-8}$ m s^{-1}, $E_a = 67.0 \pm 1.7$ kJ mol^{-1}) than for the dissociated NAA (pH 6.2, $P_d = 1.1(\pm 0.2) \times 10^{-8}$ m s^{-1}, $E_a = 51.8 \pm 1.9$ kJ mol^{-1}). The activation energy for penetration of the dissociated NAA was closely related to the stomatal density ($R^2 = 0.84$***, $P < 0.0001$) but less so for the nondissociated NAA ($R^2 = 0.30$*, $P < 0.03$). These data provide evidence for the presence of polar pathways through the sweet cherry fruit exocarp that allow water uptake by viscous flow. These pathways offer a potentially useful target for strategies to reduce water uptake and fruit cracking, provided that a technique is identified that selectively "plugs" these pathways.

KEYWORDS: Fruit cracking; cuticle; cuticular membrane; *Prunus avium* L.; stomata; water permeability

INTRODUCTION

Rain-induced cracking of sweet cherry fruit is an important limitation to crop production worldwide and is thought to be related to increased turgor resulting from water uptake into the fruit. Water uptake occurs through the fruit surface (*1*), along the pedicel/fruit juncture (*2*), and, to a yet unknown amount, through the pedicel. The mechanism of water uptake is not entirely clear, and there is some evidence suggesting that viscous flow contributes to water uptake into sweet cherry fruit (*3*).

The cuticular membrane (CM) is a lipoidal polymer that covers surfaces of leaves and fruit including sweet cherry. The CM serves as the primary barrier for transport of substances into and out of plants. Penetration across the CM may occur along two parallel pathways, a "lipophilic" and a "polar" pathway. Penetration along the lipophilic pathways occurs by sorption, diffusion, and desorption and, thus, favors lipophilic molecules. A polar pathway formed by an aqueous continuum through the CM was suggested to account for penetration of polar and charged molecules (*4*−*7*). This pathway has received renewed interest in recent years (*8*−*11*). The evidence for polar pathways is primarily circumstantial and results from penetration characteristics. These include the following: First, penetration

* To whom correspondence should be addressed. Phone: +49-345-5522642. Fax: +49-345-5527543. E-mail: moritz.knoche@landw.uni-halle.de.

10.1021/jf053220a CCC: $33.50
Published on Web 05/03/2006

favors polar and charged molecules that are excluded from the lipophilic pathway on the basis of their solubility (*7*, *8*). Second, the polar pathway is porous in nature, and hence, penetration is size selective (*9*, *11*, *12*). Third, the effect of temperature on penetration along the polar pathway is smaller than that along the lipophilic pathway (*13*). Fourth, penetration along a polar pathway formed by a liquid continuum across the CM should depend on viscosity. Fifth, polar pathways are dynamic structures that form upon hydration and orientation of polar functional groups of CM constituents, resulting in increased water permeability at high humidity (*3*, *14*, *15*). Sixth, for porous membranes, the permeability determined in the presence of a pressure gradient exceeds the permeability in self-diffusion, that is, the permeability in the absence of a pressure gradient (*13*). Also, the effect of temperature differs between osmotically driven water penetration and self-diffusion of water across a porous membrane (*13*).

In sweet cherry fruit, our early study provided evidence for the last three of the above characteristics, supporting the hypothesis that viscous flow along a polar pathway may contribute to water uptake (*3*). However, it is not known whether the other penetration characteristics of polar pathways also apply to sweet cherry fruit. We therefore investigated (i) the effect of viscosity on osmotic water uptake, (ii) the size selectivity of a polar pathway by studying the effect of the molecular weight of selected osmotica on osmotic water uptake, and (iii) the effect of temperature on penetration of the organic acid 2-(1-naphthyl)-acetic acid (NAA) in the dissociated and nondissociated form.

MATERIALS AND METHODS

Plant Material. Sweet cherry fruit [*Prunus avium* L., Adriana, Burlat, Early Rivers, Hedelfinger, Regina, and Sam, all grafted on Alkavo (*P. avium*) rootstocks] were collected at full maturity from commercial orchards near Halle and an experimental orchard of the Landratsamt Freiburg, Breisgau-Hochschwarzwald, Germany. Fruit were selected for uniformity of maturity and size on the basis of color and freedom from defects. For diffusion studies exocarp segments (ES) consisting of cuticle, epidermis, hypodermis, and some layers of mesocarp tissue were excised from the cheek region of Sam sweet cherries using a razor blade. These segments were stored in 1 g L^{-1} NaN_3 at 5 °C until use. Unless specified otherwise, water uptake experiments on whole fruit were carried out within 24 h of sampling.

Water Uptake Assays: General Procedure for Detached Fruit. Water uptake into detached sweet cherries was determined gravimetrically. Uptake was restricted to the exocarp by removing pedicels by gently pulling and sealing the resulting hole above the stony endocarp using silicone rubber (Dow Corning 3140 RTV Coating, Dow Corning Corp., Midland, MI; *2*). Following curing at ambient conditions overnight, fruit were weighed, incubated in treatment solutions for 45 min at 22 °C, removed from solutions, blotted using tissue paper, and subsequently reweighed. Thereafter, fruit were reincubated for a second time interval. Following reweighing, fruit were inspected for macroscopic cracks. Observations on fruit that cracked in the course of the experiment were excluded from data analysis. Rates of water uptake (F, g h^{-1}) were determined on an individual fruit basis from the slope of a linear regression line fitted through a plot of cumulative water uptake vs time. Coefficients of determination of representative experiments averaged $R^2 = 0.96 \pm 0.01$ ($n = 539$), indicating a constant rate of water uptake. From F, the flux J (kg m^{-2} s^{-1}) was calculated by dividing F by the fruit surface area (A, m^2; eq 1). A was estimated

$$F = AJ = AP_f(\rho \bar{V}_w/RT)\Delta\Psi \quad (1)$$

from the fruit mass assuming a density of sweet cherry fruit of 1000 kg m^{-3} and a spherical fruit shape as first approximations. In some experiments, the osmotic permeability of the exocarp (P_f, m s^{-1}) was calculated using eq 1, where $\Delta\Psi$ (MPa) represented the gradient in water potential between the osmotic potential of the treatment solution (Ψ_Π, MPa) and the water potential of the fruit (Ψ_{fruit}, MPa), ρ (kg m^{-3}) the density of water, and $\bar{V}_w/RT$ (MPa^{-1}) the quotient of the molar volume of water ($\bar{V}_w$, m^3 mol^{-1}) divided by the universal gas constant (R, m^3 MPa mol^{-1} K^{-1}) times the absolute temperature (T, K).

Ψ_{fruit} was determined on a subsample of fruit from the same batch. Briefly, fruit were incubated in a series of poly(ethylene glycol) 6000 (PEG 6000; mean molecular weight 6000; Merck Eurolab GmbH, Darmstadt, Germany) solutions of differing osmotic potential as determined by water vapor pressure osmometry (model 5520; Wescor Inc., Logan, UT). The highest PEG 6000 concentration always had a Ψ_Π lower than Ψ_{fruit}, and hence, incubation of fruit in this solution resulted in negative rates of water uptake. Ψ_{fruit} was determined by fitting a linear regression line through a plot of F vs Ψ_Π of the PEG solutions. In some experiments, relationships between water uptake and osmotic potentials of the PEG solutions were not linear. In these cases, linear regression analysis was limited to those data points that were closely spaced around the water potential of the fruit (for example, see **Figure 3**). From the regression equation obtained Ψ_Π of a hypothetical PEG solution that resulted in zero change in fruit mass was calculated. Under this condition, Ψ_Π equals Ψ_{fruit} and there is no driving force for net water uptake ($\Delta\Psi = 0$). These assays were used to investigate the effects of viscosity and molecular weight of selected osmotica on whole fruit water uptake.

Experiments. The effect of viscosity on water uptake of detached fruit was investigated using gum arabic. Preliminary experiments established that gum arabic (from acacia; Carl Roth GmbH, Karlsruhe, Germany) had a marked effect on dynamic viscosity (η), but only a small effect on osmotic potential and, hence, the driving force for water uptake. The dynamic viscosity of incubation solutions was determined using a set of Ubbelohde capillary viscosimeters (Schott AG, Mainz, Germany). Viscosities and osmotic potentials ranged from 1.3×10^{-3} to 115.9×10^{-3} Pa s and from -0.13 to -0.44 MPa at concentrations from 10 to 300 g L^{-1}, respectively. The effect of viscosity on water uptake was established in Adriana, Burlat, Early Rivers, Hedelfinger, Regina, and Sam sweet cherry. These cultivars differ in stomata count per fruit (range 143−2124 per fruit equivalent to a calculated range in stomatal density of 0.08 to 0.97 mm^{-2} for Adriana and Hedelfinger, respectively; *16*). To account for the small, but significant effect of gum arabic on the driving force for water uptake, osmotic permeabilities (P_f) were calculated from the rates of water uptake using the water potential gradient between Ψ_{fruit} determined for each cultivar (grand mean of all cultivars: $\Psi_{fruit} = -2.8$ MPa, range -2.5 to -3.2 MPa) and Ψ_Π of the respective gum arabic solution. The minimum number of single fruit replications was nine for every viscosity and cultivar.

The effect of the molecular weight of selected osmotica on water uptake was investigated in two consecutive experiments using freshly harvested fruit of Adriana, Hedelfinger, and Sam sweet cherry. First, Ψ_{fruit} values were determined for the three cultivars by incubation in PEG 6000 solutions as described above. Ψ_{fruit} values were -2.5, -2.8, and -2.7 MPa for Adriana, Hedelfinger, and Sam fruit, respectively. Subsequently, isotonic solutions of selected osmotica of differing molecular weight were prepared at the respective Ψ_{fruit} of each cultivar. The osmotica and their molecular weights were NaCl (58), glycerol (92), mannitol (182), sucrose (342), and poly(ethylene glycol) 6000 (6000). The change in fruit mass upon incubation in these solutions was determined gravimetrically as described above. The minimum number of single fruit replications was nine per osmoticum and cultivar.

Apparent fruit water potentials (ψ'_{fruit}), reflection coefficients, and size selectivity of the polar pathway were determined using detached Sam sweet cherry fruit held in storage for up to 29 d. Using stored fruit reduced day-to-day variability in the fruit water potential caused by varying growing conditions in the orchard. Storing conditions were 0.4 ± 0.1 °C, 72.2 ± 0.4% relative humidity, 17.5 ± 0.1% O_2, and 18.0 ± 0.4% CO_2. Information on the size distribution of polar pathways in the sweet cherry fruit exocarp may be obtained from ψ'_{fruit} determined by monitoring the change in fruit mass during incubation in osmotica of differing molecular weight. This hypothesis is based on the following assumption. ψ'_{fruit} should depend on the molecular weight of the osmoticum, if the osmotica penetrated the exocarp. In contrast, ψ'_{fruit} should remain constant, if there was no penetration. Using this approach,

ψ'_{fruit} values of Sam sweet cherry fruit were determined in series of concentrations using the osmotica listed above except for mannitol, which was replaced by proline (molecular weight 115) because of its higher water solubility. PEG 1500 (molecular weight 1500) was included as an additional osmoticum to fill the gap in molecular weights between sucrose (342) and PEG 6000 (6000). Experiments were carried out sequentially with a minimum number of seven single fruit observations per osmoticum and concentration. In studies on membrane transport reflection coefficients (σ, dimensionless) are often used to characterize the relative ease of movement of a solute through a membrane relative to that of a solute for which the membrane is impermeable (*17*). We assumed the sweet cherry fruit exocarp to be impermeable to the largest osmoticum PEG 6000 ($\psi_\pi = \psi'_{fruit} = \psi_{fruit}$ for PEG 6000, and hence, $\sigma = 1$) and calculated σ for the osmotica listed above relative to PEG 6000 according to eq 2.

$$\sigma = \Psi_{fruit}/\Psi'_{fruit} \quad (2)$$

Hydrodynamic radii (r, m) of the osmotica NaCl, glycerol, proline, and sucrose were calculated using the Stokes−Einstein relation and published diffusion coefficients (D, $m^2\ s^{-1}$) in H_2O (*18*−*20*; eq 3). In

$$D = kT/6\pi\eta r \quad (3)$$

this equation k equals the Boltzmann constant ($k = 1.381 \times 10^{-23}$ J K^{-1}), T the absolute temperature (T, K), and η the viscosity of water ($\eta = 0.8909 \times 10^{-3}$ kg s m^{-1} at 25 °C). Since NaCl dissociates and the hydrodynamic radius of the Na cation is larger than that of the Cl anion, calculations were based on the Na cation. Mean molecular radii of PEG 1500 and PEG 6000 were calculated from a nonlinear regression line fitted through data published for a homologous series of poly(ethylene glycol) [Table 2 in ref *21*; range in molecular weight (MW) of 400 to 8000, r ($\times 10^{-9}$ m) = $0.03(MW)^{0.50}$, $R^2 = 1.00$].

Diffusion Studies: ES. Diffusion of 2-(1-naphthyl)[1-^{14}C]acetic acid ([^{14}C]NAA; specific activity 2.3 Gbq $mmol^{-1}$, 98.7% radiochemical purity by TLC; Amersham Corp., Arlington Heights, IL) through sweet cherry ES was determined using the infinite dose technique (*22*). In this system diffusion is monitored under quasi-steady-state conditions from a dilute donor solution through an interfacing membrane into a receiver solution. ES were mounted in plexiglass holders (5 mm inner diameter) using silicone rubber (Dow Corning 3140 RTV Coating, Dow Corning Corp.) and subsequently inspected for microscopic cracks in the CM at 100× magnification. ES having microscopic cracks were discarded. The number of stomata per ES was determined by light microscopy (100×). Stomatal density (d_{sto}, mm^{-2}) was calculated by dividing the stomatal number by the cross-sectional area of the plexiglass holder. Holders with crack-free ES were mounted between two glass half-cells using silicone grease (Baysilone-Paste hochviskos; GE Bayer Silicones, Leverkusen, Germany) such that the morphological outer side of the ES faced the donor. Diffusion cells were placed in a water bath (25 °C) positioned on a multiple stirring unit. Receiver solutions were prepared using a 10 mM citric acid buffer and 1 mM NaN_3 to prevent microbial growth. The pH was adjusted to 2.2 and 6.2 using HCl and NaOH, which is 2 pH units below and above the pK_a for NAA (pK_a = 4.2), respectively. Buffer solutions used as donor solutions contained 10 μM cold NAA plus 0.7×10^5 dpm mL^{-1} [^{14}C]NAA at pH 2.2 (total NAA concentration 11 μM) or 10 μM cold NAA plus 7.3×10^5 dpm mL^{-1} [^{14}C]NAA at pH 6.2 (total NAA concentration 16 μM). Diffusion experiments were initiated by adding 5 mL of donor and receiver solution to the donor and receiver cells of the diffusion units. The time course of penetration of NAA was followed by repeated sampling of the receiver solution. Aliquots (1 mL) were removed from the receiver solutions, radioassayed by liquid scintillation spectrometry (scintillation cocktail Ultima Gold XR; PerkinElmer Life and Analytical Sciences, Boston, MA; counter: LS 6500; Beckman Instruments Inc., Fullerton, CA), and replaced by fresh buffer solution of the respective pH. Following establishment of steady-state flow at 25 °C, temperature was decreased to 5 °C and subsequently increased in 10 °C intervals up to 35 °C. Steady-state flow was established at any one temperature. Flow rates were calculated by fitting a linear regression line through a plot of cumulative NAA penetration vs time. The slope of this regression equation equaled the flow (F, dpm h^{-1}). F is related to the permeability in diffusion (P_d, m s^{-1}) by eq 4, where A

$$F = AJ = AP_d\Delta C \quad (4)$$

(m^2) represents the cross-sectional area of the ES exposed in the diffusion cell and ΔC (dpm m^{-3}) the driving force for transport, i.e., the gradient in radioactivity across the ES. Since the concentration of radioactivity in the receiver solution is negligibly low, ΔC corresponded to the concentration of radioactivity in the donor.

The temperature dependence of penetration of nondissociated (pH 2.2) and dissociated (pH 6.2) NAA was analyzed by calculating the energy of activation (E_a) from the slopes of Arrhenius plots of the natural logarithm of P_d vs the inverse of the absolute temperature. Since temperature was increased sequentially, E_a values were calculated on an individual ES basis (n = 16 ES per pH).

Statistics and Data Presentation. Data were subjected to analysis of variance (ANOVA). ANOVA (Proc Anova, Proc Glm), multiple comparisons of means, and regression analysis (Proc Reg) were carried out using the Statistical Analysis System software package (version 8.02; SAS Institute Inc., Cary, NC). Unless specified otherwise, regression analysis was performed on treatment means. The data in the figures are presented as means ± SE of the means. Where not shown, error bars were smaller than the data symbols.

RESULTS

The amount of water taken up by Sam sweet cherry fruit increased linearly with time (**Figure 1a**). Increasing the viscosity of the incubation solution by increasing the concentration of gum arabic decreased the rates of water uptake (**Figure 1a**) and permeability for osmotic water uptake (**Figure 1b**). Plotting the permeability for osmotic water uptake vs the inverse of viscosity revealed a significant linear relationship for four of the six sweet cherry cultivars investigated (**Figure 1c**, **Table 1**). There was no significant relationship between the effect of viscosity on water uptake as indexed by the slope of regression lines and stomatal number per fruit across the sweet cherry cultivars [slope (Pa m) = $[2.42(\pm 1.35) \times 10^{-14}]$(no. of stomata per fruit)] − $0.09(\pm 1.88) \times 10^{-11}$, $R^2 = 0.44$, $P < 0.15$]. In addition, viscosity had no effect on water uptake in the cultivar Adriana, which has the lowest stomatal number (**Table 1**).

Incubating Sam sweet cherry fruit in isotonic solutions of selected osmotica had a marked effect on water uptake that depended on the molecular weight of the osmoticum (**Figure 2a**). There was no water uptake from isotonic PEG 6000 solutions, but flow rates increased as the molecular weight of the osmotica decreased (**Figure 2b**). Qualitatively and quantitatively similar data were obtained for Adriana and Hedelfinger sweet cherry fruit (Weichert, data not shown).

Decreasing the osmotic potential of the incubation solution decreased the rates of water uptake into Sam sweet cherry fruit for all osmotica (**Figure 3**). At the highest concentrations equivalent to the lowest osmotic potential, negative rates of water uptake were obtained for all osmotica. Calculating the apparent fruit water potential (ψ'_{fruit}) from the concentration response for the different osmotica revealed that ψ'_{fruit} depended on the molecular weight of the osmotica (**Figure 3**). ψ'_{fruit} increased as the molecular weight of the osmotica increased up to 1500 (**Figure 4a**). A further increase in MW to 6000 had no additional effect on ψ'_{fruit}. The reflection coefficients derived from these relationships were closely related to the hydrodynamic radii of the osmotica [$\sigma = 1.0(\pm 0.0) - [10.9(\pm 0.9) \times 10^{-11}][r^{-1}\ (m^{-1})]$, $R^2 = 0.97$, $P < 0.0001$; **Figure 4b**].

Penetration of NAA through the sweet cherry fruit exocarp increased with time and temperature (**Figure 5a**). Calculating NAA permeability demonstrated that (i) P_d of the nondissociated

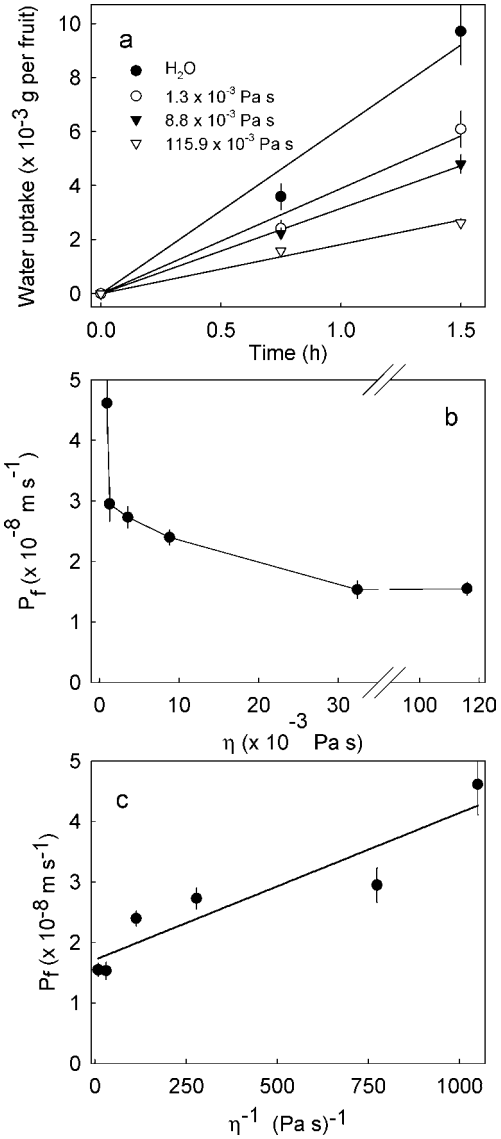

Figure 1. Effect of viscosity on water uptake through the exocarp of Sam sweet cherry fruit: (**a**) time course of water uptake, (**b**) permeability of osmotic water uptake (P_f) as affected by dynamic viscosity (η), (**c**) P_f as a function of the inverse viscosity (η^{-1}; Hagen–Poiseuille plot). For the regression equation see **Table 1**.

Table 1. Regression Equations for the Relationship between the Inverse of the Dynamic Viscosity (η^{-1}) of Aqueous Gum Arabic Solutions and the Osmotic Permeability for Water Uptake (P_f) in Fruit of Selected Sweet Cherry Cultivars[a]

cultivar	no. of stomata per fruit	regression parameters $y_0 \pm$ SE (10^{-8} m s^{-1})	regression parameters $a \pm$ SE (10^{-11} Pa m)	coeff of determination (R^2)	P
Adriana	143	1.56 ± 0.38	1.29 ± 0.70	0.46	0.14
Burlat	1679	4.41 ± 0.53	1.83 ± 0.97	0.47	0.13
Early Rivers	1268[b]	2.08 ± 0.13	1.22 ± 0.24	0.87	0.007
Hedelfinger	2124	4.57 ± 0.61	7.91 ± 1.11	0.93	0.002
Regina	1427	2.62 ± 0.15	2.70 ± 0.27	0.96	0.0006
Sam	779	1.71 ± 0.27	2.42 ± 0.49	0.86	0.008

[a] The cultivars selected differed in the number of stomata (*16*). The regression model was P_f (m s^{-1}) = $y_0 + a[\eta^{-1}$ (Pa s)$^{-1}]$. [b] Knoche, unpublished data.

NAA (pH 2.2) was about 1 order of magnitude higher than that of the dissociated species (pH 6.2) and (ii) temperature had a larger effect on P_d of the nondissociated than that of the

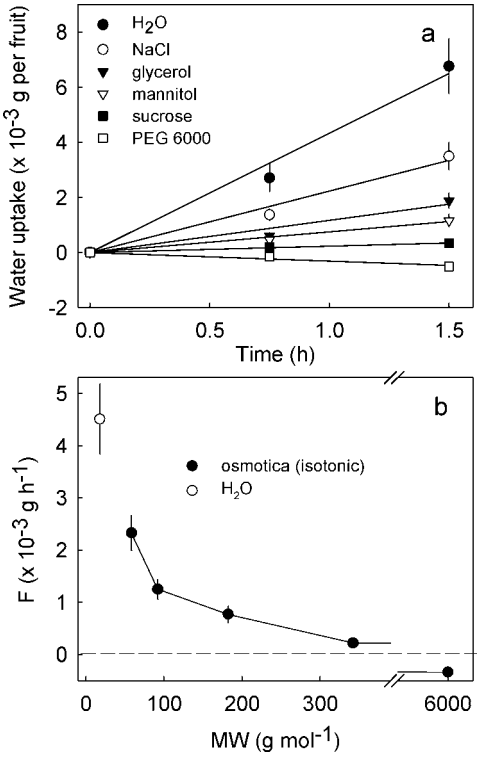

Figure 2. Effect of osmotica of differing MW on water uptake through the exocarp of Sam sweet cherry fruit: (**a**) time course of water uptake, (**b**) flow rate of water (F) as a function of the molecular weight of the osmotica. All solutions were isotonic to the water potential of the sweet cherry fruit ($\Psi_\Pi = \Psi_{fruit}$). Deionized water served as the control.

dissociated NAA (**Figure 5b**). Arrhenius plots were linear at both pH values, but the slopes of the Arrhenius plots were significantly higher at pH 2.2 than at pH 6.2, indicating a higher energy of activation (E_a) for P_d of the nondissociated than the dissociated NAA (67.0 ± 1.7 vs 51.8 ± 1.9 kJ mol^{-1} at pH 2.2 vs 6.2, respectively; **Figure 5c**). Furthermore, plotting the energy of activation vs stomatal density revealed that E_a for penetration of the dissociated species of NAA was more closely related to the stomatal density ($R^2 = 0.84$***, $P < 0.0001$) than that of the nondissociated species ($R^2 = 0.30$*, $P < 0.03$; **Figure 5d**).

DISCUSSION

Evidence for Polar Pathways. Our data provide further evidence for the presence of polar pathways through the exocarp of sweet cherry fruit. This conclusion is based on the following arguments.

First, osmotic water permeability was linearly related to the inverse of viscosity (**Figure 1c**, **Table 1**). Theoretically, viscous flow through a polar pathway formed by an aqueous continuum across the exocarp may be described by Hagen−Poiseuille's law where the flow rate (F) through a tube of radius (r) is given by

$$F = -\frac{\pi r^4}{8\eta}\frac{dP}{dx} \quad (5)$$

In this equation dP/dx represents the drop in hydrostatic pressure along the tube, i.e., the porous pathway, and η the viscosity of the solution. Rearranging eq 5 demonstrates that, for a given geometry of the tube and driving force, F is inversely related to the viscosity of the solution. We used gum arabic to vary the viscosity, and gum arabic had a small, but significant effect on osmotic potential that confounded its effect on viscosity. This

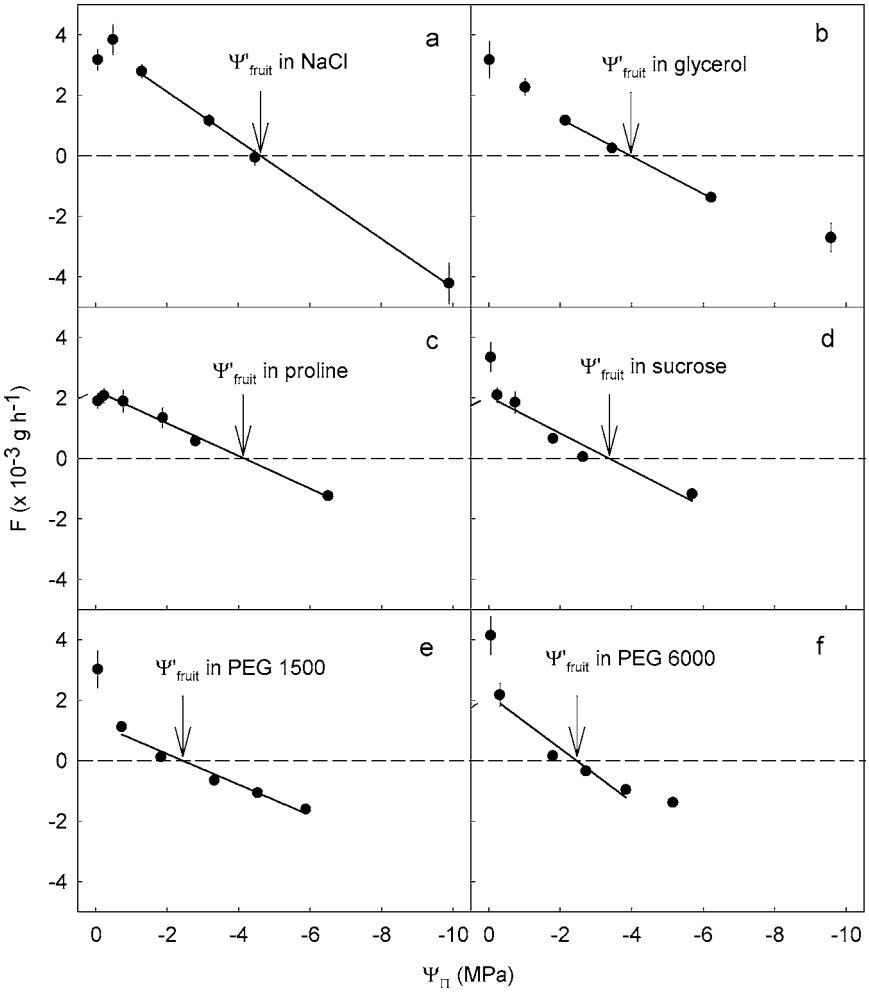

Figure 3. Effect of the osmotic potential (Ψ_Π) of solutions containing osmotica of differing MW on the flow rate of water (*F*) through the exocarp of Sam sweet cherry fruit. The osmotica were (**a**) NaCl, (**b**) glycerol, (**c**) proline, (**d**) sucrose, (**e**) PEG 1500, and (**f**) PEG 6000. Arrows indicate the apparent fruit water potential (Ψ'_{fruit}) when incubated in the respective osmoticum.

effect, however, was corrected for by calculating P_f values from flow rates and respective driving forces. The relationships thus obtained were linear and significant for four of the six cultivars investigated as would be predicted from the Hagen−Poiseuille law (**Figure 1c**, **Table 1**). The absence of a significant relationship in Adriana sweet cherry fruit is most likely accounted for by the low number of stomata and, hence, their markedly smaller contribution to total water uptake (*16*). At present we do not know why viscosity accounted for only 47% of water uptake in Burlat. On the basis of the number of stomata per fruit, we would have expected a significant relationship and a high coefficient of determination. Potential reasons include differences in (i) the size of the stomatal apparatus and/or (ii) the structure and composition of the CM that result in different numbers and dimensions of polar pathways per unit surface area.

The second argument is based on the finding that the apparent water potential of sweet cherry fruit increased as the molecular weight of the osmotica increased up to about 1500 (**Figure 4a**). This is evidence for size-dependent penetration along the polar pathway that excluded molecules having a molecular weight ≥1500. Since the osmotica used were polar, the size-selective penetration must have occurred through a polar pathway.

Third, infinite dose diffusion studies using the organic acid NAA established that (i) the permeabilities and (ii) the activation energies for NAA penetration through the sweet cherry fruit exocarp were higher for the nondissociated than for the dissociated species of NAA (**Figure 5**). The nondissociated species of NAA is more lipophilic and, hence, is expected to penetrate the cuticle via the lipophilic pathway. In contrast penetration of the more polar dissociated species should take place to a larger extent along the polar pathway.

These arguments together with our earlier finding that osmotic permeability for water exceeded the permeability in self-diffusion (*3*, *13*) and that temperature dependence of water transport was higher in self-diffusion than in osmotic water uptake (*3*) provide definitive evidence for the presence of a liquid continuum across the sweet cherry fruit exocarp that serves as a polar pathway for penetration of polar molecules including water.

Nature of the Polar Pathway. Polar pathways occur in higher density in the CM above anticlinal cell walls (*23*, *24*), above guard and accessory cells and the cuticular ledges of the stomatal apparatus (*4*−*7*, *11*, *24*, *25*), and around the base and on the surface of trichomes (*10*, *11*, *23*). The sweet cherry fruit CM has no trichomes, and thus, the latter pathway can be excluded for sweet cherry fruit.

In sweet cherry fruit polar pathways are associated with the stomatal apparatus and the CM between stomata. Information on the stomatal route is readily obtained from the slope of the regression line fitted through plots of E_a vs d_{sto}, which is lower for the dissociated than the nondissociated species (**Figure 5d**). Also, in this and our earlier studies positive correlations were obtained between the rates of water uptake through the sweet cherry fruit exocarp of a given cultivar and stomatal density

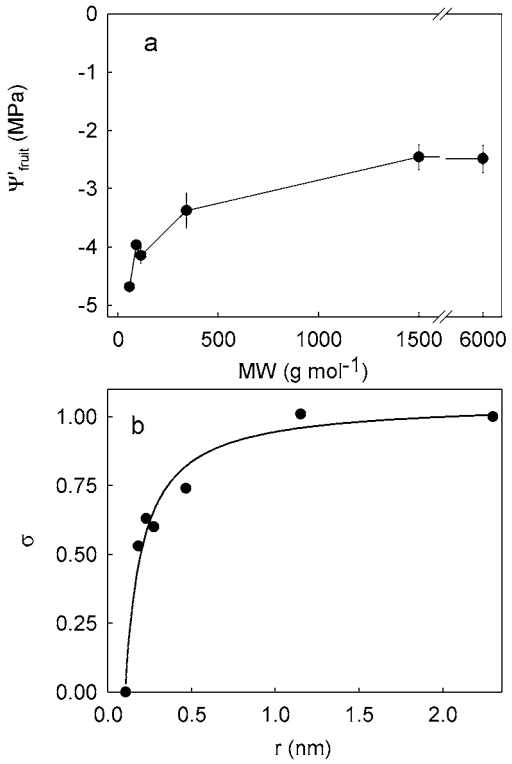

Figure 4. (**a**) Apparent water potential (Ψ'_{fruit}) as affected by the MW of the osmoticum. The osmotica were NaCl, glycerol, proline, sucrose, PEG 1500, and PEG 6000. (**b**) Reflection coefficients (σ) as a function of the hydrodynamic radii of the osmotica. The osmotica and their respective MWs and radii (r) were NaCl, MW = 58, $r_{Na^+} = 0.18 \times 10^{-9}$ m; glycerol, MW = 92, $r = 0.23 \times 10^{-9}$ m; proline, MW = 115, $r = 0.28 \times 10^{-9}$ m; sucrose, MW = 342, $r = 0.47 \times 10^{-9}$ m; PEG 1500, MW = 1500, $r = 1.2 \times 10^{-9}$ m; and PEG 6000, MW = 6000, $r = 2.3 \times 10^{-9}$ m. The regression equation was $\sigma = 1.0(\pm 0.0) - [10.9(\pm 0.9) \times 10^{-11}][r^{-1}\ (m^{-1})]$, $R^2 = 0.97$, $P < 0.0001$.

(*3*). The nature of the flow associated with stomata is not clear at present. Viscous flow through the open stomatal pore should be prevented by the wetting characteristics of the fruit surface and the high surface tension of aqueous solutions (*16*, *26*). Also, scanning electron microscopy studies revealed that pores of a significant fraction of stomata are partially occluded (M. J. Bukovac, personal communication). However, viscous flow as a water film lining the pore may provide for a liquid continuum allowing penetration to bypass the CM (*27*, *28*). This mechanism would also account for an effect of viscosity on penetration but not for the size selectivity of the polar pathway as determined by the apparent fruit water potential in different osmotica (**Figures 3** and **4**). Alternatively, a higher density of polar pathways in the CM above guard and accessory cells and cuticular ledges reported in the literature would explain significant relationships between water uptake and stomatal density (*3*) or between the temperature dependence of NAA penetration and stomatal density (**Figure 5d**). For the latter substance E_a per stoma was lower for the dissociated than the nondissociated NAA.

Evidence for the presence of polar pathways in the CM between the stomata comes from the *y* axis intercepts of plots of water uptake vs stomatal density (*3*) or the activation energy of NAA penetration vs stomatal density (**Figure 5d**). These intercepts may be interpreted as the respective water uptake or E_a for NAA penetration through a hypothetical astomatous sweet cherry fruit segment. E_a for penetration of the dissociated species

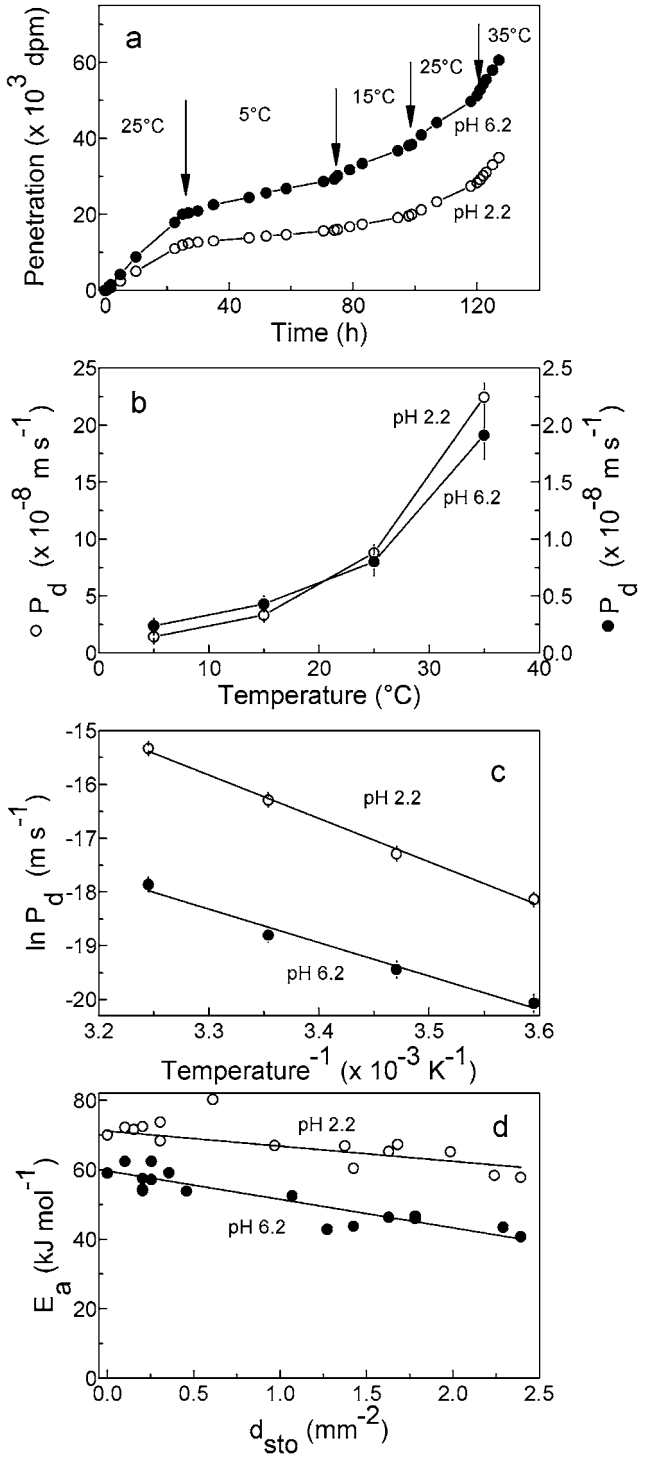

Figure 5. Effect of temperature on NAA diffusion through excised exocarp segments of mature Sam sweet cherry fruit: (**a**) time course of penetration at pH 2.2 and 6.2, (**b**) effect of temperature on NAA permeability (P_d) at pH 2.2 and 6.2 (note the different scales of the *y* axes for pH 2.2 and 6.2), (**c**) Arrhenius plot [the mean energy of activation (E_a) calculated from the slope of the regression line was 67.0(±1.7) and 51.8(±1.9) kJ mol^{-1} at pH 2.2 and 6.2, respectively], (**d**) E_a for NAA diffusion at pH 2.2 or 6.2 as a function of stomatal density (d_{sto}). The regression equations were (pH 2.2) E_a (kJ mol^{-1}) = –4.4(±1.8)[d_{sto} (mm^{-2})] + 71.2(±2.3), $R^2 = 0.30$*, $P < 0.03$, and (pH 6.2) E_a (kJ mol^{-1}) = –8.2(±1.0)[d_{sto} (mm^{-2})] + 59.7(±1.2), $R^2 = 0.84$***, $P < 0.0001$.

is again lower than that of the nondissociated species as would be expected if a polar pathway were involved in penetration of the dissociated compound.

It may be argued that microscopic cracks in the CM of mature sweet cherry fruit serve as "polar pathways" for penetration. These cracks are infiltrated by aqueous fluorescent dye solutions even in the absence of a surfactant (*29*), indicating that they serve as high-flux pathways for water uptake. This uptake would likely be affected by the viscosity of the incubation solution. However, penetration through microscopic cracks would not be size selective, and hence, the observed size selectivity (**Figures 3** and **4**) cannot be accounted for. Also, ES used in the infinite dose diffusion studies on NAA penetration were crack free as indexed by microscopic inspection at 100× magnification (**Figure 5**). These arguments exclude microscopic cracks as the size-selective polar pathway in the sweet cherry fruit CM.

Schönherr (*12*) estimated equivalent radii of polar pores from direct determinations of solute penetration, and from comparing permeability for osmotic water uptake with that for self-diffusion using the procedure by Nevis (*30*). The equivalent pore radii derived ranged from 0.4 to 0.5 nm and were in remarkable agreement with direct measurements of mean distances of polymer chains in tomato cutin determined by X-ray diffraction (mean distances 0.45 and 1.0 nm; *31*). In our experiments the hydrodynamic radius of the smallest nonpenetrating osmoticum (PEG 1500 with $\sigma = 1$) was 1.15 nm and that of the largest penetrating osmoticum (sucrose with $\sigma = 0.74$) was 0.47 nm, suggesting a size exclusion limit of the polar pathway between 0.47 and 1.15 nm. Estimating equivalent pore radii using the procedure by Nevis (*30*) as adopted by Schönherr (*12*) and published data on permeability for osmotic water uptake and for self-diffusion through the sweet cherry fruit exocarp (*3*) yielded pore radii between 0.53 and 1.00 nm. These calculations demonstrate that the polar pathway across the sweet cherry fruit exocarp must be similar to those previously reported for other plant species. It should be pointed out that the above estimates represent only mean equivalent pore radii and do not imply uniform cylindrical pores that traverse the CM perpendicular to the surface. In a real system, radii will be variable and depend on the extent of hydration, presence of counterions, and, possibly, strain of the CM (*12*, *14*).

Conclusions. The data presented provide definitive evidence for the presence of polar pathways across the sweet cherry fruit exocarp that allow rapid water uptake into the fruit. In sweet cherry fruit, polar pathways are associated with stomata, but also occur in the CM between stomata. These pathways offer a potentially useful target for strategies to reduce water uptake and ultimately fruit cracking, provided that a technique can be identified that selectively "plugs" these pathways, thereby eliminating rapid water uptake by viscous flow. Beyer et al. (*32*) and Weichert et al. (*33*) recently demonstrated that some inorganic salts including $AlCl_3$ and $FeCl_3$ decreased permeability for osmotic water uptake and, hence, cracking of sweet cherry fruit. The decrease in water permeability was most likely caused by formation of complex viscous aluminum or iron oxides and hydroxides. On the basis of the evidence provided in this paper, it may be hypothesized that this reaction occurred within the polar pathways identified in this and our earlier study (*3*). Studies are in progress in our laboratory to test this hypothesis. A better understanding of the mechanism of water uptake and the effect of salts thereon is a prerequisite for developing strategies to reduce fruit cracking in sweet cherry using substances that have a more acceptable ecotoxicological profile than the salts used in the study cited above.

ABBREVIATIONS USED

A, surface area; CM(s), cuticular membrane(s); d_{sto}, number of stomata per unit surface area; E_a, energy of activation; ES, exocarp segment; *F*, flow rate of water; *J*, flux of water per unit area and time; MW, molecular weight; P_d, permeability coefficient for self-diffusion; P_f, permeability coefficient for osmotic water uptake; PEG, poly(ethylene glycol); Ψ'_{fruit}, apparent fruit water potential; Ψ_{fruit}, fruit water potential; Ψ_Π, osmotic potential; σ, reflection coefficient.

ACKNOWLEDGMENT

We thank Hubert Schneider, Kurt Ehm, and Wolfgang Meyer for providing fruit samples and Matthias Hinz, Evelyn, and Ruth Richter for technical assistance.

LITERATURE CITED

(1) Beyer, M.; Knoche, M. Studies on water transport through the sweet cherry fruit surface: V. Conductance for water uptake. *J. Am. Soc. Hortic. Sci.* **2002**, *127*, 325−332.

(2) Beyer, M.; Peschel, S.; Knoche, M.; Knörgen, M. Studies on water transport through the sweet cherry fruit surface: IV. Regions of preferential uptake. *HortScience* **2002**, *37*, 637−641.

(3) Beyer, M.; Lau, S.; Knoche, M. Studies on water transport through the sweet cherry fruit surface: IX. Comparing permeability in water uptake and transpiration. *Planta* **2005**, *220*, 474−485.

(4) Franke, W. Role of guard cells in foliar absorption. *Nature* **1964**, *202*, 1236−1237.

(5) Franke, W. Mechanisms of foliar penetration of solutions. *Annu. Rev. Plant Physiol.* **1967**, *18*, 281−300.

(6) Neumann, S.; Jacob, F. Aufnahme von α-Aminoisobuttersäure durch die Blätter von *Vicia faba* L. *Naturwissenschaften* **1968**, *55*, 89−90.

(7) Schönherr, J.; Bukovac, M. J. Preferential polar pathways in the cuticle and their relationship to ectodesmata. *Planta* **1970**, *92*, 189−201.

(8) Schönherr, J. Calcium chloride penetrates plant cuticles via aqueous pores. *Planta* **2000**, *212*, 112−118.

(9) Schönherr, J.; Schreiber, L. Size selectivity of aqueous pores in astomatous cuticular membranes isolated from *Populus canescens* (Aiton) Sm. leaves. *Planta* **2004**, *219*, 405−411.

(10) Schreiber, L. Polar paths of diffusion across plant cuticles: new evidence for an old hypothesis. *Ann. Bot.* **2005**, *95*, 1069−1073.

(11) Schlegel, T. K.; Schönherr, J.; Schreiber, L. Size selectivity of aqueous pores in stomatous cuticles of *Vicia faba* leaves. *Planta* **2005**, *221*, 648−655.

(12) Schönherr, J. Water permeability of isolated cuticular membranes: The effect of pH and cations on diffusion, hydrodynamic permeability and size of polar pores in the cutin matrix. *Planta* **1976**, *128*, 113−126.

(13) House, C. R. Water transport in cells and tissues. In *Monographs of the Physiological Society*, Number 24; Davson, H., Greenfield, A. D. M., Whittam, R., Brindley, G. S., Eds.; Edward Arnold (Publishers) Ltd.: London, Great Britain, 1974; pp 88 and 190.

(14) Schönherr, J.; Schmidt, H. W. Water permeability of plant cuticles−dependence of permeability coefficients of cuticular transpiration on vapor pressure saturation deficit. *Planta* **1979**, *144*, 391−400.

(15) Schreiber, L.; Skrabs, M.; Hartmann, K. D.; Diamantopoulos, P.; Simanova, E.; Santrucek, J. Effect of humidity on cuticular water permeability of isolated cuticular membranes and leaf disks. *Planta* **2001**, *214*, 274−282.

(16) Peschel, S.; Beyer, M.; Knoche, M. Surface characteristics of sweet cherry fruit: stomata number, distribution, functionality and surface wetting. *Sci. Hortic.* **2003**, *97*, 265−278.

(17) Nobel, P. S. *Physicochemical and Environmental Plant Physiology*; Academic Press: San Diego, 1999.

(18) Derlacki, Z. J.; Easteal, A. J.; Edge, A. V. J.; Woolf, L. A.; Roksandic, Z. Diffusion coefficients of methanol and water and the mutual diffusion coefficient in methanol−water solutions at 278 and 298 K. *J. Phys. Chem.* **1985**, *89*, 5318−5322.

(19) Lide, D. R. *Handbook of Chemistry and Physics*, 76th ed.; CRC Press Inc.: Boca Raton, FL, 1995; pp 6−257.
(20) Longsworth, L. G. Diffusion measurements, at 25 °C, of aqueous solutions of amino acids, peptides and sugars. *J. Am. Chem. Soc.* **1953**, *75*, 5705−5709.
(21) Atha, D. H.; Ingham, K. C. Mechanism of precipitation of proteins by polyethylene glycols. *J. Biol. Chem.* **1981**, *256*, 12108−12117.
(22) Bukovac, M. J.; Petracek, P. D. Characterizing pesticide and surfactant penetration with isolated plant cuticles. *Pestic. Sci.* **1993**, *37*, 179−194.
(23) Franke, W. Ectodesmata and foliar absorption. *Am. J. Bot.* **1961**, *48*, 683−691.
(24) Franke, W. Über die Beziehungen der Ektodesmen zur Stoffaufnahme durch Blätter. III. Mitteilung: Nachweis der Beteiligung der Ektodesmen an der Stoffaufnahme durch Blätter mittels radioaktiver Stoffe. *Planta* **1964**, *61*, 1−16.
(25) Jyung, W. H.; Wittwer, S. H.; Bukovac, M. J. The role of stomata in the foliar absorption of Rb by leaves of tobacco and tomato. *Proc. Am. Soc. Hortic. Sci.* **1965**, *86*, 361−367.
(26) Schönherr, J.; Bukovac, M. J. Penetration of stomata by liquids. Dependence on surface tension, wettability, and stomatal morphology. *Plant Physiol.* **1972**, *49*, 813−819.
(27) Eichert, T.; Goldbach, H. E.; Burkhardt, J. Evidence for the uptake of large anions through the stomatal pores. *Bot. Acta* **1998**, *111*, 461−466.
(28) Eichert, T.; Burkhardt, J. Quantification of stomatal uptake of ionic solutes using a new model system. *J. Exp. Bot.* **2001**, *52*, 771−781.
(29) Peschel, S.; Knoche, M. Characterization of microcracks in the cuticle of developing sweet cherry fruit. *J. Am. Soc. Hortic. Sci.* **2005**, *130*, 487−495.
(30) Nevis, A. H. Water transport in invertebrate peripheral nerve fibres. *J. Gen. Physiol.* **1958**, *41*, 927−958.
(31) Luque, P.; Bruque, S.; Heredia, A. Water permeability of isolated cuticular membranes: A structural analysis. *Arch. Biochem. Biophys.* **1995**, *317*, 417−422.
(32) Beyer, M.; Peschel, S.; Weichert, H.; Knoche, M. Studies on water transport through the sweet cherry fruit surface: VII. Fe^{3+} and Al^{3+} reduce conductance for water uptake. *J. Agric. Food Chem.* **2002**, *50*, 7600−7608.
(33) Weichert, H.; v. Jagemann, C.; Peschel, S.; Knoche, M.; Neumann, D.; Erfurth, W. Studies on water transport through the sweet cherry fruit surface: VIII. Effect of selected cations on water uptake and fruit cracking. *J. Am. Soc. Hortic. Sci.* **2004**, *129*, 781−788.

Received for review December 23, 2005. Revised manuscript received April 4, 2006. Accepted April 5, 2006. This study was supported by a grant from the Deutsche Forschungsgemeinschaft.

JF053220A